International Conference on Mathematics and Computational Methods Applied to Nuclear Science and Engineering (M&C 2011)
Rio de Janeiro, RJ, Brazil, May 8-12, 2011, on CD-ROM, Latin American Section (LAS) / American Nuclear Society (ANS)
ISBN 978-85-63688-00-2

APPLICATION OF SENSITIVITY ANALYSIS TO A SIMPLIFIED COUPLED NEUTRONIC THERMAL-HYDRAULICS TRANSIENT IN A FAST REACTOR USING ADJOINT TECHNIQUES

L. Gilli *, D. Lathouwers, J.L. Kloosterman, T.H.J.J. van der Hagen
Delft University of Technology, Faculty of Applied Sciences
Department of Radiation, Radionuclides and Reactors
Physics of Nuclear Reactors
Mekelweg 15, 2629 JB Delft, The Netherlands
l.gilli@tudelft.nl

ABSTRACT

In this paper a method to perform sensitivity analysis for a simplified multi-physics problem is presented. The method is based on the Adjoint Sensitivity Analysis Procedure which is used to apply first order perturbation theory to linear and nonlinear problems using adjoint techniques. The multi-physics problem considered includes a neutronic, a thermo-kinetics, and a thermal-hydraulics part and it is used to model the time dependent behavior of a sodium cooled fast reactor.
The adjoint procedure is applied to calculate the sensitivity coefficients with respect to the kinetic parameters of the problem for two reference transients using two different model responses, the results obtained are then compared with the values given by a direct sampling of the forward nonlinear problem.
Our first results show that, thanks to modern numerical techniques, the procedure is relatively easy to implement and provides good estimation for most perturbations, making the method appealing for more detailed problems.

Key Words: Uncertainty Analysis, ASAP, multi-physics problems

1. INTRODUCTION

The design of future nuclear reactor systems such as Generation IV reactors starts with simulations performed using computer codes. In order to assess the reliability of these simulations, we need to estimate the uncertainty associated with their results. This uncertainty is caused by two main contributions: first, the fact that a system is described adopting a simplified mathematical model and using numerical approximations and second, the lack of knowledge of the input data of the problem [1].

The first type of uncertainty introduces the need for validation and verification tools while the second one involves understanding how the uncertainty on the input data (represented by the material composition, the geometry, and by the boundary conditions) is propagated. In the present work we deal with this type of uncertainty applying a propagation technique to a simplified coupled model.

*Corresponding author.

Many propagation methods have been developed during the past decades, a main distinction can be made between statistical and deterministic techniques. The concept behind the first group is very straightforward: the same simulation is performed with different input sets randomly generated according to their statistical distribution. The result is a set of output values which contains information about the total output uncertainty. This kind of method has the main advantage of giving very accurate results but at the price of a very high computational cost which increases with the size of the input data set. On the other side, deterministic methods have been developed by means of mathematical models aiming to create faster tools sacrificing part of the accuracy.

A popular technique in the latter group is the Sensitivity Analysis (SA) which is based on the mathematical derivation of a linear relationship between the output of the simulation and each of the input parameters. The SA is usually performed using adjoint methods [3] which can be used to find a general expression for the variation of an output with respect to an input parameter at a very low computational cost. Adjoint methods have been widely applied to reactor physics problems and they have recently been implemented in modern codes used to perform uncertainty analysis for future nuclear reactors. Unfortunately these applications have been mostly limited to linear problems: mainly steady state [2] but more recently also time-dependent [4]. One of the few applications of an adjoint method to a nonlinear coupled problem can be found in a old code [5] developed at the Idaho National Laboratory.

The main aim of this paper is to propose the application of an adjoint method to a coupled problem, in particular a time-dependent simulation in which a simplified neutronic model is coupled to a thermo-kinetic/thermal-hydraulic one. The method used to perform this task is the Adjoint Sensitivity Analysis Procedure (ASAP), developed by Cacuci [6], which is directly applied to a discretized numerical model. The paper contains the mathematical derivation of the simulation model and the description of the application of the adjoint method followed by its application to two transients calculated for a reference system, a sodium cooled fast reactor (a Russian BN800). The results obtained with the adjoint method are finally compared with the ones obtained using exact calculations.

2. DESCRIPTION OF THE MULTI-PHYSICS PROBLEM

2.1 Definition of the Coupled Model

The problem considered for the application of the ASAP is a model describing the time-dependent behavior of a sodium fast reactor. The reference configuration used is the BN800, a sodium cooled fast breeder reactor under construction in Russia, whose details have been taken from an IAEA benchmark [7] (its main characteristics are summarized in Table I). The neutronic part of the coupled problem is described using a point-kinetic model

$$\begin{aligned} \frac{dP}{dt} &= \frac{\rho(t)-\beta}{\Lambda}P + \sum_{k}^{K}\lambda_k C_k \\ \frac{dC_k}{dt} &= -\lambda_k C_k + \frac{\beta_k}{\Lambda}P \end{aligned} \tag{1}$$

where the reactivity (the term which introduces the nonlinear coupling in the neutronic part) is considered as the sum of three different contributions

$$\rho(t) = \rho_{ext}(t) + \delta\rho_D(t) + \delta\rho_C(t) \tag{2}$$

the external reactivity is provided as an external input of the model while the Doppler (D) and coolant (C) ones represent the temperature dependent feedback mechanisms. These reactivities are determined by spatial averaging the temperature field

$$\delta\rho_D = \alpha_D \frac{1}{V_f} \int\int dr dz 2\pi r \left[\varphi_D(r,z)\left(T_f(r,z) - T_{rf}\right)\right] \tag{3}$$

$$\delta\rho_C = \alpha_C \frac{1}{H} \int dz \left[\varphi_C(r,z)\left(T_c(r,z) - T_{rc}\right)\right] \tag{4}$$

φ_D and φ_C are spatial weighing functions and α_D and α_C the first order reactivity coefficients, modeled around a reference temperature T_r, using the fuel and the coolant averaged temperatures.

$$\begin{aligned} \alpha_D &= \left(\frac{\partial\rho}{\partial\bar{T}_f}\right)_{T_{rf}} \\ \alpha_C &= \left(\frac{\partial\rho}{\partial\bar{T}_C}\right)_{T_{rc}} \end{aligned} \tag{5}$$

The kinetic parameters used in the point-kinetic model and the reactivity coefficients have been obtained using the ERANOS2.2 code [8] for the complete heterogeneous 3D model.

In order to model the temperature fields required to calculate the feedbacks, the reactor domain is divided in N regions. Each of them is considered as constituted by a number n_p of pins of the same kind: in each pin the volumetric heat produced is transfered, across the cylindrical fuel and cladding, to the sodium coolant which is supposed to have a fixed inlet temperature. Axial conduction along the pin is neglected which means that each pin is modeled using a set of radial energy conservation equations. In figure 1 the reference geometry for the thermo-kinetic problem is shown. For each region N we use the following equation for the fuel

$$\rho_f c_{p,f} \frac{\partial T_f^z}{\partial t} = \frac{1}{r}\frac{\partial}{\partial r}\left(r k_f\left(T_f^z\right)\frac{\partial T_f^z}{\partial r}\right) + f^z(P) \tag{6}$$

where the superscript z refers to the position along the vertical axis and $f^z(P)$ is a shape function used to describe the distribution of the volumetric power. This function is supposed to be distributed as the fundamental neutronic solution of an equivalent homogeneous cylindric core. Similarly, for the cladding we have

$$\rho_{cl} c_{p,cl} \frac{\partial T_{cl}^z}{\partial t} = \frac{1}{r}\frac{\partial}{\partial r}\left(r k_{cl}\left(T_{cl}^z\right)\frac{\partial T_{cl}^z}{\partial r}\right) \tag{7}$$

The thermodynamic and heat transport properties of the fuel and the cladding have been characterized using correlations present in [9] while the main properties for the sodium coolant have been taken in [10]. The boundary conditions used for the thermo-kinetic problem are

$$\begin{aligned}
\left.\frac{\partial T_f^z}{\partial r}\right|_{r=0} &= 0 \\
k_f(T_f^z)\left.\frac{\partial T_f^z}{\partial r}\right|_{Rf} &= h_g(T_{cl}^z|_{Rf+\delta_g} - T_f^z|_{Rf}) \\
R_f\ k_f(T_f^z)\left.\frac{\partial T_f^z}{\partial r}\right|_{Rf} &= (R_f+\delta_g)\ k_{cl}(T_{cl}^z)\left.\frac{\partial T_{cl}^z}{\partial r}\right|_{Rf+\delta_g} \\
k_{cl}(T_{cl}^z)\left.\frac{\partial T_{cl}^z}{\partial r}\right|_{Rs} &= h_c(T_c(z))(T_c(z) - T_{cl}^z|_{Rs})
\end{aligned} \tag{8}$$

where the second boundary condition is used to model the temperature drop across the gap between the fuel and the cladding (the heat transfer coefficient for the gap has been taken from [9]) and the last condition couples the heat transfer across the pin with the removal performed by the coolant. Its temperature is determined by the following energy conservation equation, used for each equivalent channel

$$A_c\rho c_{pc}\left[\frac{\partial T_c}{\partial t} + w\frac{\partial T_c}{\partial z}\right] - 2\pi R_s n_p h_c(T_c)(T_{cl}(R_s,z) - T_c) = 0 \tag{9}$$

where A_c is the equivalent flow area, a fixed coolant velocity is considered and the boundary condition is given by a fixed coolant inlet temperature. The solution for each equivalent region is coupled to the point-kinetic model through the integrals 5.

Finally we define a response for the problem, response which depends on the solution of the system just derived. This can be modeled as the following linear functional

$$\begin{aligned}
R = &\int_0^{t_f} w_P(t)P(t)dt + \int_0^{t_f}\int\int 2\pi r w_f(r,z,t)T_f(r,z,t)drdzdt + \\
&+\int_0^{t_f}\int\int 2\pi r w_{cl}(r,z,t)T_{cl}drdzdt + \int_0^{t_f}\int w_c(z,t)T_c(z,t)dzdt
\end{aligned} \tag{10}$$

The response is quite generic and can be modified by means of response functions w. As an example, the centerline temperature at $z = z_r$ and at the final time t_f can be defined as

$$\begin{aligned}
w_P(t) = w_{cl}(r,z,t) = w_c(z,t) &= 0 \\
w_f(r,z,t) &= \frac{1}{2\pi r}\delta_r(r)\delta_t(t-t_f)\delta_z(z-z_r)
\end{aligned} \tag{11}$$

With the introduction of the response the time-dependent problem has been defined. In the next subsection a general description of the code developed to solve the direct problem is given.

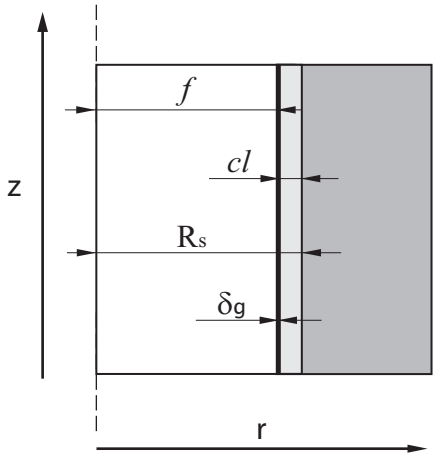

Figure 1: Reference geometry for the thermo-kinetic problem.

2.2 Numerical Solution of the Problem

The main framework of the code has been written in C language using the linear algebra modules of the Gnu Scientific Libraries [11] and the linear and nonlinear solvers of the SUNDIALS suite [12]. All the spatial derivatives introduced by the energy conservation equations have been approximated using a finite volume scheme. A uniform mesh has been defined for the fuel pin and coolant and linear interpolation has been used to determine surface values between each volume. After the discretization of the spatial problem we obtain a system of coupled ODEs

$$\begin{aligned} \frac{d\mathbf{u}(t)}{dt} &= \mathrm{L}(\boldsymbol{\alpha}, \mathbf{u}, t) \\ \mathbf{u}(0) &= \mathbf{U}_0 \end{aligned} \tag{12}$$

the vector $\boldsymbol{\alpha}$ contains the input parameter set for the nonlinear problem while the vector $\mathbf{u}$ is composed of the unknowns coming from the point-kinetic equations and the average values of the temperature on each volume of the discretized domain. The time dependent problem has been discretized using a second order Backward Differential Formula (BDF) which expresses the time derivative using a second order Lagrange polynomial, approximating it using a three point interpolation. Furthermore an adaptive step size control has been implemented in order to achieve a small truncation error. The nonlinear system arising from the previous approximation is solved using the KINSOL component from the SUNDIALS suite, a solver for nonlinear algebraic systems based on Newton-Krylov techniques.

The model introduced in the previous section has been solved using 50 volumes for each of the 30 radial equations and 150 volumes for the coolant channel. The absolute error for the time integration has been set to 10^{-6}.

Table I: Main characteristics of the BN800 model

Λ (s)	4.00E-07	r_{pin} (cm)	0.348
α_d (pcm/K)	-6.87E-01	r_{clad} (cm)	0.055
α_v (pcm/K)	1.23E-01	d_{gap} (cm)	0.0001
H(m)	0.91	P(MW)	2100
λ_1 (1/s)	0.0124	β_1 (-)	0.00009
λ_2 (1/s)	0.0305	β_2 (-)	0.000853
λ_3 (1/s)	0.111	β_3 (-)	0.0007
λ_4 (1/s)	0.301	β_4 (-)	0.0014
λ_5 (1/s)	1.14	β_5 (-)	0.0006
λ_6 (1/s)	3.01	β_6 (-)	0.00055

3. DESCRIPTION OF DASAP

In order to perform sensitivity analysis of the problem we implemented the Discrete Adjoint Sensitivity Analysis Procedure (DASAP), introduced in [6], which can be used to apply first order perturbation theory to any nonlinear time-dependent problem. The first step to perform first order sensitivity analysis is the application of the definition of Gateaux Derivative (G.D.) to such a system. First we express the parameter and the unknown vectors as perturbation around a reference state

$$\begin{aligned} \boldsymbol{\alpha} &= \boldsymbol{\alpha}_0 + \delta\boldsymbol{\alpha} \\ \mathbf{u} &= \mathbf{u_0} + \delta\mathbf{u} \end{aligned} \tag{13}$$

the reference state is defined as the solution of the unperturbed system defined by the equation 12. In this way the first order variation of each unknown can be defined as the solution of the linear equation

$$\begin{aligned} \frac{d\delta\mathbf{u}(t)}{dt} &= \frac{\partial \mathrm{L}}{\partial \boldsymbol{\alpha}}(\boldsymbol{\alpha}_0, \mathbf{u}_0, t)\delta\boldsymbol{\alpha} + \frac{\partial \mathrm{L}}{\partial \mathbf{u}}(\boldsymbol{\alpha}_0, \mathbf{u}_0, t)\delta\mathbf{u} \\ \delta\mathbf{u}(\mathbf{0}) &= \delta\mathbf{U_0} \end{aligned} \tag{14}$$

the G.D. can be seen as a directional derivative of a functional, with the direction given by the variation of the input parameters and unknowns. All the operators in the previous equation are linear and depend on the solution of the reference nonlinear problem $\mathbf{u_0}$. The same operation can be applied to the functional introduced to define a response for our model

$$\begin{aligned} R &= \mathrm{R}(\boldsymbol{\alpha}, \mathbf{u}) \\ DR &= \frac{\partial \mathrm{R}}{\partial \boldsymbol{\alpha}}(\boldsymbol{\alpha_0}, \mathbf{u_0}) \cdot \delta\boldsymbol{\alpha} + \frac{\partial \mathrm{R}}{\partial \mathbf{u}}(\boldsymbol{\alpha_0}, \mathbf{u}_0) \cdot \delta\mathbf{u} \end{aligned} \tag{15}$$

where the response variation is obtained as the sum of a direct term, depending on the input perturbation, and an indirect contribution depending on the perturbation of the unknowns. The first order perturbation of the response corresponding to a perturbation on the model input could be already obtained solving equation 14 for a single perturbation and substituting the solution in 15. However, this direct method, known as the Forward Sensitivity Analysis Procedure, would be too expensive in case one would need to determine a large set of sensitivity coefficients. The DASAP has been derived as a way to overcome this computational cost introducing a solution for equations 14 and 15 by means of an adjoint problem. It is possible to show [6] that a first order variation of the response can be obtained using the following expression

$$DR = \frac{\partial \mathrm{R}}{\partial \boldsymbol{\alpha}}(\boldsymbol{\alpha_0}, \mathbf{u_0}) \cdot \delta\boldsymbol{\alpha} - \int_0^{t_f} \mathbf{u}^*(t) \cdot \left[\frac{\partial \mathrm{L}}{\partial \boldsymbol{\alpha}} (\boldsymbol{\alpha}_0, \mathbf{u_0}) \, \delta\boldsymbol{\alpha} \right] dt - \mathbf{u}^*(t=0) \cdot \delta\mathbf{U}_0 \tag{16}$$

where $\mathbf{u}^*$ is defined as the solution of the adjoint problem

$$-\frac{d\mathbf{u}^*}{dt} - \left[\frac{\partial \mathrm{L}}{\partial \mathbf{u}} (\boldsymbol{\alpha}_0, \mathbf{u_0}) \right]^T \mathbf{u}^* = \frac{\partial \mathrm{R}}{\partial \mathbf{u}} \tag{17}$$

the choice of the initial value conditions for this equation requires a more detailed discussion, in general one has to choose them in order to eliminate all the bilinear terms coming from the definition of the adjoint problem. Once this solution is known one can obtain the first order variation with respect to any input parameter simply by performing few scalar products and integrations. Some important aspects must be stressed about the method and, in particular, about the adjoint problem

- The adjoint of the time derivative operator involves a change of sign. Considering that most of the responses are represented by a Dirac delta localized at the final time, one can show that the most convenient way to integrate the adjoint problem is going backward in time.
- Its definition involves the knowledge of the Jacobian matrix of the system (the partial derivative of the operator with respect to the unknowns).
- In case of nonlinear problems this Jacobian matrix is time dependent and its coefficients are determined by the reference solution.

The first and the second points imply that in order to solve the adjoint problem one would need to store the complete original reference solution. Furthermore, as it has been shown in [4], the adjoint solution for the point-kinetic equation may become very stiff and requires the use of an adaptive time stepping approach: in the presence of large scale problems all these points could lead to memory issues. A way to overcome this problem is to implement a check-pointing scheme [12] which is intended to reduce the memory requirement paying a longer computational time. In such a scheme the reference solution is divided into intervals and a first run of the nonlinear code stores the value of the solution at the boundaries of each interval. The adjoint integration is then done after re-calculating the forward solution on each interval using the value stored at the checkpoints as the initial condition. This procedure is repeated until the last check point is reached and, since after each interval the direct solution is deleted, the amount of memory required by the code is reduced considerably. Figure 2 shows the scheme of the method.

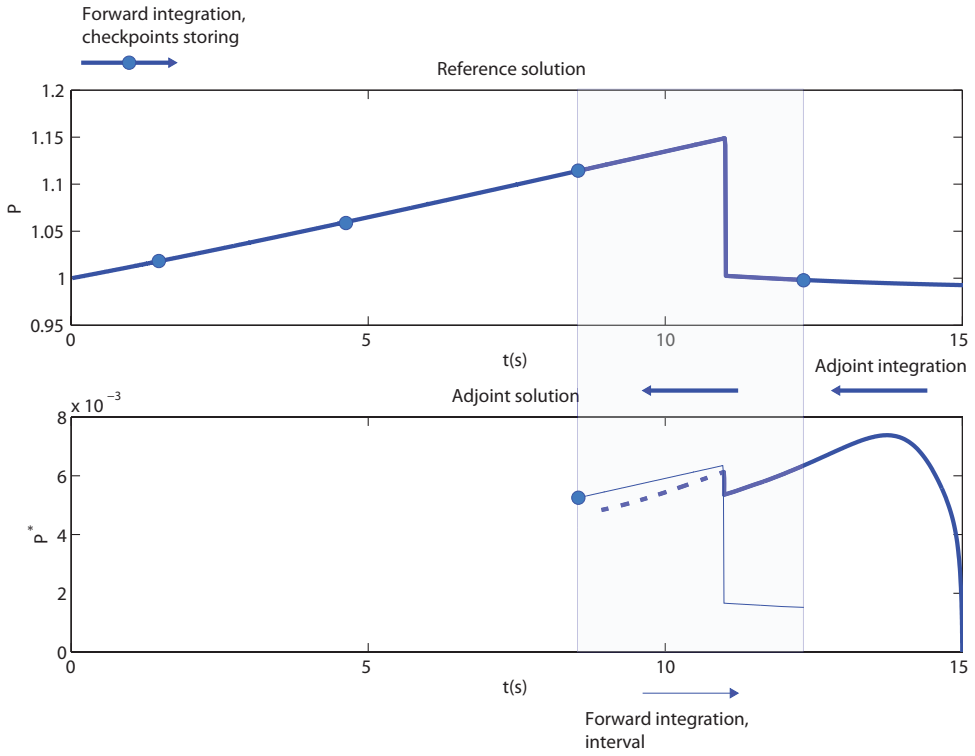

Figure 2: Check-pointing scheme required for the adjoint calculation.

The adjoint code implemented for the present work uses a second order BDF scheme for the time stepping together with the linear DENSE module from the SUNDIALS package to solve the linear algebraic system. The same nonlinear solver used for the reference problem is used to perform the nonlinear interval integration, the coefficients of the problem are obtained from this direct solution using a second order interpolating polynomial.

The Jacobian information of the nonlinear operator was derived analytically and verified using a finite difference approximation, however our future aim is to implement an Automatic Differentiation technique [13] which can be used to automatically obtain any derivative information for large scale problem where it would be hard to obtain analytically. Within the reactor physics

field, an example of the application of AD is given in [14] where the technique has been used to perform perturbation theory for coupled models.

4. SENSITIVITY ANALYSIS FOR TWO REFERENCE TRANSIENTS

The DASAP method has been applied to the coupled model introduced before with the aim of benchmarking its performances with a simplified nonlinear multi-physics problem. The responses considered for this problem are the reactor power (response 1) and the maximum inner cladding temperature (response 2) at a certain point of the transient. Two different initiating events have been introduced to perform this study: a positive reactivity insertion and a loss of coolant flow. The first transient describes the evolution of the system associated to the following external reactivity insertion

$$\rho_{ext}(t) = \begin{cases} \frac{t}{t_s}\rho_{max}; & t \leq t_s \\ 0; & t > t_s \end{cases} \tag{18}$$

where $\rho_{max} = 0.1\beta$ and $t_s = 20s$. Figure 3 shows the solution for the power and the maximum cladding temperature. The power rise associated to the positive reactivity is followed by a drop driven by the Doppler mechanism. After an oscillating period a new steady state configuration is reached. The clad temperature drops as well since a constant flow and inlet temperature are provided.

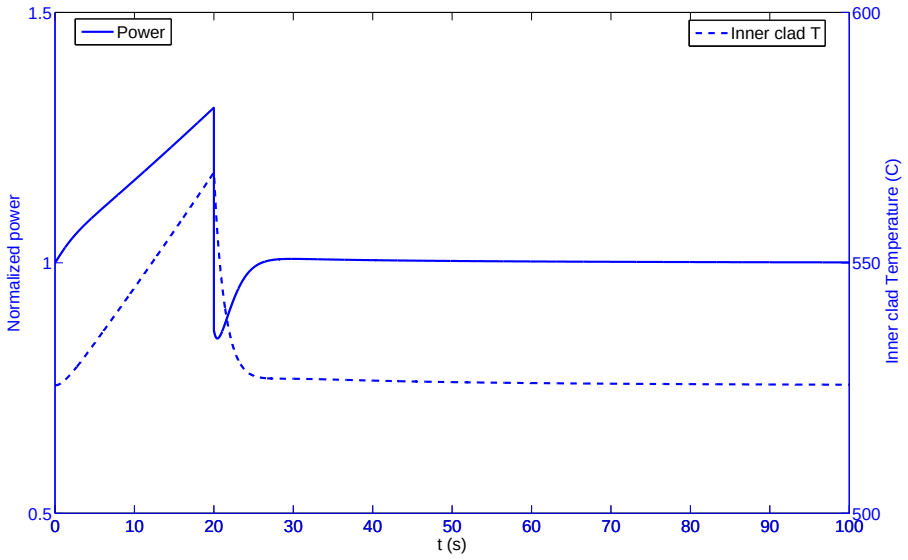

Figure 3: First reference transient: linear reactivity insertion between t=0s and t=20s. Power and clad temperature profiles.

The second transient is driven by a loss of flow, modeled using the following time-dependent velocity

$$w(t) = w(0)\,[0.97\exp(-0.0776t) + 0.03] \tag{19}$$

the velocity decreases exponentially, dropping to approximately 1/30 of the initial value after 60 seconds. In figure 4 the two solutions for this transient are plotted. The clad temperature increases immediately causing an increase of the average fuel temperature. After the first second of transient the Doppler reactivity contribution becomes larger than the coolant one because of its larger magnitude. This leads to a power decrease which ends when the pin reaches a steady temperature.

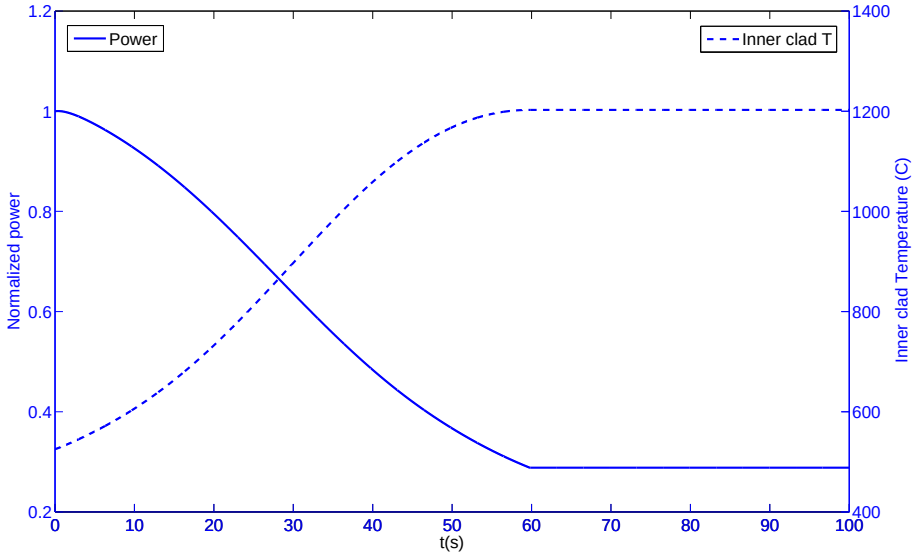

Figure 4: Second reference transient: loss of coolant flow. Power and clad temperature profiles.

These two reference solutions have been calculated using the parameter set collected in Table I. The DASAP has been applied to each of the solutions to perform sensitivity analysis with respect to the Doppler and coolant reactivity coefficients and to the kinetic parameters β_k and λ_k. It must be pointed out that once the adjoint problem is solved, the sensitivity coefficients for any kind of input perturbation (material, thermal-hydraulics properties) can be obtained very easily by performing few integrations and scalar products.

Table II contains the sensitivity coefficients obtained for the two reference transients and the two responses, localized at $t = 50s$. Each sensitivity coefficient gives a first order estimation about the influence of the associated input parameter variation on the final response. For the first transient it emerges that when the response considered is the reactor power the most important parameters are β_2, λ_2 and β_4, λ_4 followed by the Doppler reactivity coefficient. If we consider the maximum clad temperature instead, the Doppler coefficient becomes the most important. On the other side the second transient is very sensitive to both reactivity coefficients while the 2nd, 3rd and 4th play the most important role among the precursors.

Table II: Sensitivity coefficient set for the two transients and the two responses at t = 50s

$S(\%/\%)$	I transient		II transient	
Response	1	2	1	2
α_D	-0.014393	-0.037121	-0.378240	-0.132089
α_C	0.000135	0.000622	0.160093	0.056458
λ_1	-0.010226	-0.002629	-0.005885	-0.003533
λ_2	-0.055398	-0.01406	0.021745	-0.003386
λ_3	0.002612	0.0038765	0.035134	0.01199
λ_4	-0.016005	0.006142	0.024888	0.010247
λ_5	-0.003569	-0.000522	0.002234	0.001128
λ_6	-0.000739	-0.000206	0.000460	0.000388
β_1	0.011534	0.003205	0.020047	0.008194
β_2	0.080641	0.024199	0.046356	0.028367
β_3	-0.002108	0.003249	-0.033916	-0.010211
β_4	-0.031233	-0.012427	-0.026872	-0.010513
β_5	0.006214	0.000200	-0.002310	-0.001149
β_6	0.001009	0.000211	-0.000467	-0.000391

The validity of the first order perturbation method has been finally assessed comparing its results with the exact values obtained sampling the code for every single perturbation. Tables III and IV contain the perturbations for the first transient while Tables V and VI refer to the second.

Table III: ASAP vs Sampled values for the first transient, final power

Case 1	Response 1, δP (-)					
t=10s	2%			10%		
	Direct	DASAP	err (%)	Direct	DASAP	err (%)
α_D	-0.000496	-0.00049	0.69	-0.0023824	-0.00246	3.22
α_C	1.08E-05	1.07E-05	0.25	5.19E-05	5.37E-05	3.38
β_1	-0.00037	-0.000367	0.10	-0.00184	-0.001843	0.05
β_6	0.00019	0.000191	0.43	0.000944	0.000955	1.16
λ_1	3.72E-04	3.75E-04	0.83	0.001865	0.00187	0.44
λ_6	-1.676E-04	-1.65E-04	1.35	-8.29E-04	-8.27E-04	0.26
t=50s	2%			10%		
α_D	-0.0002871	-0.00028209	-1.77	-0.0016507	-0.00141047	-17.03
α_C	-1.3E-06	-1.24E-06	4.61	-5.7E-06	-6.2E-06	7.93
β_1	-0.0002025	-0.00020042	-1.03	-0.0010058	-0.00100212	-0.37
β_6	-1.4E-05	-1.449E-05	3.38	-6.85E-05	-7.245E-05	5.45
λ_1	0.0002215	0.00022606	2.02	0.0011559	0.00113032	-2.26
λ_6	2.06E-05	1.9782E-05	-4.13	1.032E-05	9.891E-05	-4.34

Table IV: ASAP vs Sampled values for the first transient, max clad temperature

Case 1	Response 2, δT (K)					
t=10s	2%			10%		
	Direct	DASAP	err (%)	Direct	DASAP	err (%)
α_D	-0.02683	-0.02669	-0.54	-0.13386	-0.1334	0.32
α_C	0.00062	0.000627	1.11	0.0.0026	0.0026266	1.01
β_1	-0.03004	-0.02993561	-0.34	-0.15167	-0.14967803	1.33
β_6	-0.02579	-0.0249908	-3.19	-0.13127	-0.124954	5.05
λ_1	0.02846	0.02882969	1.28	0.14442	0.14414846	0.18
λ_6	0.02565	0.0270076	5.03	0.12152	0.13504	10.01
t=50s	2%			10%		
α_D	-0.39348	-0.408334	3.64	-1.70632	-2.04167	16.42
α_C	0.00687	0.00684304	-0.39	0.03428	0.0342152	-0.19
β_1	-0.02872	-0.02891366	0.67	-0.14521	-0.1445683	-0.44
β_6	-0.00223	-0.002262	1.41	-0.01146	-0.01131	-1.32
λ_1	0.03572	0.03525132	-1.33	0.18046	0.1762566	-2.38
λ_6	0.00218	0.002322	6.11	0.01099	0.01161	5.34

Table V: ASAP vs Sampled values for the second transient, final power

Case 2	Response 1, δP (-)					
t=10s	2%			10%		
	Direct	DASAP	err (%)	Direct	DASAP	err (%)
α_D	-0.0007	-0.000688	-1.38	-0.0032	-0.00344	7.02
α_C	0.00027	0.000274	1.40	0.001358	0.00137	0.86
β_1	-2.13E-04	-2.15E-04	0.89	-1.077E-03	-1.07E-03	-0.26
β_6	6.532E-06	6.83E-06	-3.4	3.542E-05	3.42E-05	-3.69
λ_1	0.000228	0.000232	-1.68	0.001196	0.00116	3.28
λ_6	-6.5E-06	-6.78E-06	-3.81	-3.5E-05	-3.39E-05	2.24
t=50s	2%			10%		
α_D	-0.00219	-0.00227	3.45	-0.01023	-0.01135	9.85
α_C	0.000959	0.000961	0.13	0.00483	0.0048	-0.57
β_1	-3.56E-05	-3.5E-05	-0.94	-0.0001773	-0.00018	-0.43
β_6	2.86E-06	2.76E-06	-3.7	1.45E-05	1.38E-05	-5.15
λ_1	0.0001241	0.0001203	-3.18	0.000625	0.000601	-3.98
λ_6	-2.56E-06	-2.8E-06	8.64	-1.52E-05	-1.401E-05	-8.57

In each table the comparison between the DASAP prediction and the exact value has been performed for two perturbation magnitudes (2% and 10% variation of the reference values) and for two different final instants ($t = 10s$ and $t = 50s$). The discrepancy between the values calculated with the DASAP and the ones obtained with the sampling method can be explained either by the presence of higher order perturbation components (neglected by the first order theory) or by the accumulation of truncation errors generated performing the forward and the

Table VI: ASAP vs Sampled values for the second transient, max clad temperature

Case 2	Response 2, δT (K)					
t=10s	2%			10%		
	Direct	DASAP	err (%)	Direct	DASAP	err (%)
α_D	-0.10136	-0.0975302	-3.93	-0.48243	-0.487651	1.07
α_C	0.0394	0.0404986	2.71	0.2024	0.202493	0.05
β_1	-0.05348	-0.0527098	-1.46	-0.26259	-0.26354	0.36
β_6	0.00067	0.000656	-2.13	0.00316	0.00328	3.66
λ_1	0.0533	0.05497	3.04	0.27033	0.27486	1.65
λ_6	-0.00047	-0.000496	5.24	-0.00262	-0.00248	-5.52
t=50s	2%			10%		
α_D	-3.2281	-3.17014	-1.83	-14.4049	-15.8507	9.12
α_C	1.3562	1.354984	-0.09	6.8672	6.77492	-1.36
β_1	-0.0843	-0.0848	0.58	-0.4252	-0.42396	-0.29
β_6	0.0092	0.009304	1.12	0.0482	0.04652	-3.61
λ_1	0.1988	0.1966	-1.08	0.9312	0.983	5.30
λ_6	-0.00983	-0.009374	-4.86	-0.0454	-0.04687	3.14

adjoint time integrations. This accumulation becomes important when the output perturbation magnitude is comparable to the time integration accuracy, for the transients considered this is always the case for the $6th$ precursor. Comparing the errors corresponding to a 2% and a

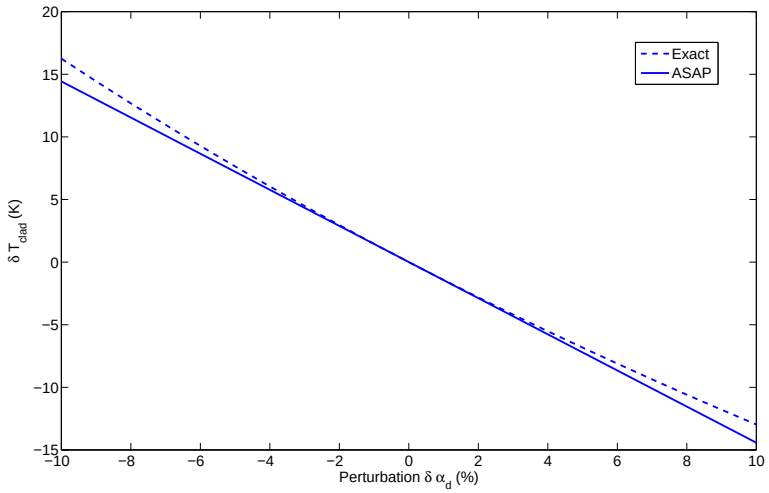

Figure 5: Linear prediction obtained with DASAP vs sampled values for clad temperature at the end of the second transient (t=50s)

10% perturbation gives a rough estimation about how higher order components are propagated throughout the model, i.e. how far is the real solution from the linear assumption. Increasing the magnitude of the perturbation makes the linear approximation introduced by equation 14

less valid, figure 5 shows this effect for the second response of the second transient. As one may expect, the Doppler reactivity coefficient is the parameter for which higher order perturbation effects are propagated more, on the other hand the behavior for the coolant coefficient and the kinetic parameters is almost linear. For the transients and the responses considered, the variation of the output due to the perturbation of the input parameter set can be estimated, most of the times, with a very good accuracy (the tables show the good performance of the method). In such cases the ASAP is one of the best options to propagate uncertainties due to its low computational cost. But in general, there may be parameters or situations for which applying this method would lead to considerable errors, a more extended investigation about the performances of the ASAP with different transients, responses and more complicated models is therefore needed.

5. CONCLUSIONS

The Discretized Adjoint Sensitivity Analysis Procedure has been applied to a simplified multi-physics problem. The discretized approach facilitates the implementation of the method to any existing code since it only requires the knowledge of the Jacobian information of the nonlinear problem, information which can be used to define the adjoint system from an algebraic point of view, avoiding any analytical formulation. The first order derivative data can be derived using approximations as the finite difference method or using exact methods like the Automatic Differentiation approach.

The code written to implement the method performed well when applied to the two reference transients introduced in the present paper, providing a good estimation for all the perturbations considered. This sensitivity analysis has been limited to few input parameters but an extension to a larger set of input data, as the one related to the material and thermal-hydraulics properties, would be straightforward. From the numerical point of view, the second order adaptive time stepping scheme reduces the time integration error and represents a good way to solve the stiff adjoint problem. In addition, the modularity of the code and the presence of a check-pointing scheme make a possible application to larger scale systems easier. The work will continue in this direction, adding more details and increasing the size of the nonlinear model and investigating about the validity range of the technique. We are currently working with the development of a multi-region Improved Quasi-static Method which will be used to have a better description of the neutronic problem.

ACKNOWLEDGEMENTS

The authors acknowledge the Nuclear Research and consultancy Group (Petten, the Netherlands) for their financial support.

REFERENCES

1. M.N. Avramova and K.N. Ivanov. Verification, validation and uncertainty quantification in multi-physics modeling for nuclear reactor design and safety analysis. *Progress in Nuclear Energy.*, **52**, pp. 601-614 (2010).

2. International Evaluation Co-operation. *Uncertainty and Target Accuracy Assessment for Innovative Systems Using Recent Covariance Data Evaluations*. OECD, Paris & France (2008).

3. M.L. Williams. *CRC Handbook for Nuclear Reactors Calculations vol III - Perturbation Theory for Nuclear Reactor Analysis*. CRC Press, Boca Raton & United States (1986).

4. W.F.G. van Rooijen and D. Lathouwers. Sensitivity Analysis for Delayed Neutron Data. *Annals of Nuclear Energy.*, **35**, pp. 2186-2194 (2008).

5. C.V. Parks and P.J. Maudlin. Application of Differential Sensitivity Theory to a Neutronic/Thermal-hydraulic Reactor Safety Code. *Nuclear Technology.*, **54**, pp. 38-53 (1981).

6. D.G. Cacuci. *Sensitivity and Uncertainty Analysis, Volume 1: Theory*. Chapman and Hall CRC, Boca Raton & United States (2003).

7. J. K. Fink and L. Leibowitz. Evaluation of benchmark calculations on a fast power reactor core with near zero sodium void effect *IAEA-TECDOC-731* (1994).

8. G. Rimpault, D. Plisson, J. Tommasi, R. Jacqmin. The Eranos Code and Data System for Fast Reactor Neutronic Analyses *Proceedings of the 2002 PHYSOR Conference* (2002).

9. A. Waltar and A. Reynolds. *Fast Breeder Reactors*. Pergamon Press, New York & United States (1981).

10. J. K. Fink and L. Leibowitz. Thermodynamic and Transport Properties of Sodium Liquid and Vapor *ANL/RE-95/2* (1995).

11. M. Galassi, J. Davies, J. Theiler, B. Gough, G. Jungman, P. Alken, M. Booth, F. Ross. *GNU Scientific Library Reference Manual - Third Edition*. Network Theory Ltd & United Kingdom (2009).

12. A. C. Hindmarsh, P. N. Brown, K. E. Grant, S. L. Lee, R. Serban, D. E. Shumaker, C. S. Woodward. SUNDIALS: Suite of Nonlinear and Differential/Algebraic Equation Solvers. *ACM Transactions on Mathematical Software.*, **31(3)**, pp. 363-396 (2005).

13. A. Griewank. *Evaluating Derivatives: Principles and Techniques of Algorithmic Differentiation. Frontiers in Applied Mathematics, vol. 19.*. SIAM & Philadelphia (2000).

14. B.T. Rearden and J.E. Horwedel. Automatic Differentiation with Code Coupling and Applications to SCALE Modules. *Proceedings of the 2007 M&C+SNA Conference* (2007).